Co-gasification of biomass and coal in a top-lit updraft fixed bed gasifier : syngas composition and its interchangeability with natural gas for combustion applications

Co-gasification of Biomass and Coal in a Top-Lit Updraft fixed bed gasifier: Syngas Composition and its Interchangeability with Natural Gas for Combustion Applications

Quintero-Coronel D A[1,3]; Lenis-Rodas Y A[2], Corredor L[1], Perreault, P[4]; Bula A[1]; Gonzalez-Quiroga A[1]*

[1]UREMA Research Unit, Department of Mechanical Engineering, Universidad del Norte, Barranquilla, Colombia

[2]Department of Mechanical Engineering, Institución Universitaria Pascual Bravo, Medellin, Colombia

[3]GITYD Research Unit, Department of Mechanical Engineering, Universidad Francisco de Paula Santander, Ocaña, Colombia

[4]Sustainable Energy, Air and Water Technology (DuEL) Group, University of Antwerp, Antwerp, Belgium

Corresponding author*: arturoq@uninorte.edu.co

Abstract

The co-gasification of biomass and coal is a promising approach for efficiently integrating the unique advantages of different gasification feedstock with syngas production. Additionally, syngas from the co-gasification of locally available biomass and coal could supplement the natural gas used in household and industrial burners. The top-lit updraft gasifier features a moving ignition front that starts at the top and propagates downward through the solids bed, while air enters from the bottom and the gas product flows upwards. This study assesses the co-gasification performance of palm kernel shell and high-volatile bituminous coal in a top-lit updraft fixed bed gasifier using 70, 85, and

100 vol % biomass and equivalence ratios ranging from 0.26 to 0.34. The results indicate that the ignition front propagates faster and is more uniform as the biomass volume increases. Micro GC analysis revealed that the H_2/CO ratio remained in the range of 0.57-0.59, 0.49-0.51, and 0.42-0.46 for experiments with 70, 85, and 100 vol % biomass, respectively. A gas interchangeability analysis showed that syngas-natural gas blends with up to 15 vol % of syngas could combust in atmospheric natural gas burners without modifications. Thus, the top-lit updraft gasifier shows excellent potential for the co-gasification of coal and biomass. Further research on this technology should explore steam as a gasification agent to enhance the syngas energy content and continuous solids feeding.

Keywords: TLUD, gasification, synthesis gas, gas interchangeability, updraft gasifier, gas industry

Nomenclature

a	correction coefficient for individual hydrocarbons	
A_T	cross-sectional area	m^2
AF	Air-Fuel ratio	
AF_s	stoichiometric Air-Fuel ratio	
C	mass percentage of atomic carbon	% wt
CCE	Carbon Conversion Efficiency	%
CGE	Cold Gas Efficiency	%
C_{pot}	combustion potential	
dafb	dry-ash-free basis	
db	dry basis	
d_{pc}	coal particle size	Mm
d_r	relative density	
FC	Fixed Carbon	% wt

HVBC	High-Volatile Bituminous Coal	
HHV	High Heating Value	kJ kg^{-1}
HHV_g	High Heating Value of gas	MJ m^{-3}
IW	Wobbe Index	MJ m^{-3}
IW_c	corrected Wobbe Index	MJ m^{-3}
K_1	correction factor 1	
K_2	correction factor 2	
LHV	Lower Heating Value	kJ kg^{-1}
LHV_g	Lower Heating Value of gas	MJ m^{-3}
LOHC	Liquid Organic Hydrogen Carrier	
$\dot{m}_f$	fuel mass flow rate	kg s^{-1}
NG	Natural Gas	
PKS	Palm Kernel Shell	
Q_a	air volumetric flow	Nm^3 s^{-1}
T	temperature	°C
t	time	S
TGA	Thermogravimetric Analysis	
TLUD	Top-Lit Updraft	
T_m	maximum temperature	°C
U	gas factor 1	
u_f	ignition front propagation velocity	mm s^{-1}
v	gas factor 2	
VM	Volatile matter	% wt
VP_c	coal Volume Percentage	% v v^{-1}
v_s	air superficial velocity	m s^{-1}

x_{Ash}	ash content	% wt
Y	dry gas yield	$Nm^3\,kg^{-1}$
y_i	molar fraction of compound i.	
Δx	distance between consecutive thermocouples	Mm
Φ	equivalence ratio	
ρ_b	bulk density	$kg\,m^{-3}$

Introduction

Biomass-coal co-gasification takes advantage of the renewable character and high reactivity of biomass and the availability and high energy content of coal. Therefore, syngas from the co-gasification of locally available solid fuels should be considered next to natural gas and green hydrogen as complementary gaseous fuels. This study presents experimental results for the co-gasification of Palm Kernel Shell (PKS) and High-Volatile Bituminous Coal (HVBC), focusing on syngas composition and its interchangeability with natural gas. The gasifier is a Top-Lit Updraft or TLUD, a vertically oriented fixed bed in which the ignition front moves from the top to the bottom while the syngas flows upward through the bed of char and ashes [1]. Moving grate furnaces and cookstoves use the TLUD operation mode [2]–[4]. This study evaluates the syngas composition for PKS-HVBC blends, two solid fuels highly available in Colombia. The study evaluates the ignition front propagation velocity, temperature profiles at several axial locations, cold gas efficiency, carbon conversion efficiency, and the lower heating value of the syngas. As a distinguishing feature, the study also assesses the syngas integration in domestic or industrial combustion applications via a gas interchangeability analysis with different natural gas references.

Energy supply reliable and affordable that allows enhancing the living standards of the humans must be joined to strategies to mitigate adverse environmental impacts [5]. Fuel derived from petroleum, natural gas, and coal corresponds to the principal fuels used for energy transformation. Using these

fuels to generate heat and power releases significant amounts of greenhouse gasses, which cause environmental and health problems [6]. Biomass, a potential carbon-neutral fuel, could supplement traditional fossil fuels [7].

Colombian coal reserves, classified as anthracite and bituminous coal, reached 4554 proved Mt in 2019 [8]. These coal reserves would last 170 years, while Colombian petroleum and natural gas would run out within 7 and 15 years, respectively, based on the current consumption rate [9]. Additionally, Colombia produces nearly 29 Mt/yr of residual biomass from sugar cane, rice husk, coffee husk, oil palm, and other crops with a primary energy potential of 12000 MWh/yr [10]. The oil palm industry produces significant amounts of residual biomass. Studies show that processing 1.0 t of fresh palm fruits results in 0.07 t of empty fruit bunches, 0.103 t of fibers, and 0.012 t of PKS [11]. PKS distinguishes by a relatively high Lower Heating Value (LHV) of 18 MJ kg^{-1} [12], [13].

The syngas mainly consists of CO, H_2, CH_4, CO_2; however, when air is the gasification agent, the syngas contains large amounts of N_2 [14], which could produce higher amounts of NOx when the syngas burns at relatively high temperatures [15]. In addition, the nitrogen content presents in the feedstocks also contributes to NOx formation. NOx emissions contribute to global warming and harm human health because they produce nausea, headache, and irritation to the eye and throat [15]. However, NOx formation from biomass gasification is lower than that formed from fossil fuel gasification [15]. Therefore, syngas obtained from biomass-fossil fuels co-gasification processes could reduce NOx emissions. The syngas has applications for heat and power generation but also chemicals and fuels. Gasification is nowadays a widely recognized biomass conversion process. However, its main drawbacks are excessive tar production [16], seasonal dependency, and the broad size distribution and variable composition of solids fuels [17]. Although coal is a fossil fuel, its co-gasification with biomass can reduce its environmental impact while alleviating the seasonal dependence issue [18]. The syngas obtained by co-gasification combines the properties of biomass

and coal. Additionally, studies report that biomass enhances the overall reactivity of coal due to its relatively high volatiles content, which improves the rate of heterogeneous reactions [19].

Fluidized and fixed beds are typical gasifiers used in the co-gasification of biomass and coal [20]. Fluidized bed gasifiers handle feedstocks with a wide particle size distribution. However, the obtained syngas has excessive tar content, and ash melting could affect fluidization quality. On the other hand, fixed bed gasifiers can produce syngas with lower tar content, although their use is limited to small-scale applications, i.e., lower than 2 MWe [21]. Some studies report the co-gasification of diverse biomasses and coals in fluidized bed [16], [18], [22]–[24], downdraft fixed bed [19], [25], [26], and entrained flow gasifiers [27]. These works mainly study syngas composition, coal and biomass properties, blend composition, tar reduction, and synergistic effects, while syngas applications remain less explored.

In this study, we use a TLUD fixed bed gasifier to co-gasify PKS and HVBC. The obtained syngas passes through a bed of char and ashes produced by the downward-moving ignition front. Published studies also refer to the TLUD operation as inverted downdraft [28], [29], reverse downdraft [30]–[32], and reverse combustion [33]. TLUD-related applications are biochar [34], syngas [35], [36], and combined biochar-syngas production [28], [37], [38]. Due to its relatively low construction costs and convenience for small-scale applications, TLUD gasifiers can potentially provide fundamental data for the design and operation of moving grate furnaces and fixed bed gasifiers for solid waste [4], [39], [40], and biomass [2], [41].

Air is the most common oxidizer used in TLUD gasifiers, producing syngas with an LHV in the range of 2-5 MJ m^{-3} [28], [37]. Some studies report the increase of CO and H_2 contents with increasing air superficial velocity while presenting an opposite trend for CO_2 and CH_4 [30], [35], [38]. Likewise, high operation temperature in the TLUD gasifier increases CO and H_2 content, enhances tar conversion, and promotes syngas production. In addition, some studies point out that the energy content of the syngas rises with an increase in the inner diameter of the TLUD for a fixed air

superficial velocity, as was observed in [42] and confirmed by Perez et al. [43]. The latter study noted an increase in syngas quality because a higher diameter enhanced the adiabaticity of the gasifier. The studies mentioned above have tested the biomass gasification in TLUD gasifiers; nevertheless, the co-gasification of coal and biomass remains less explored. Therefore, this study contributes to closing the lack of experimental work in this area.

This article is organized as follows. The first sections describe the feedstock properties, the experimental setup, and the experimental conditions. Subsequently, the gas sampling procedure, the experimental procedures, and the gas interchangeability analysis are presented. Next, the values obtained in the experiments are used to describe the gasification regime in the TLUD gasifier by assessing the temperature profiles, the ignition front propagation velocity, and the equivalence ratio in the process. Then, the syngas compositions and the performance of the TLUD are discussed based on the syngas LHV, cold gas efficiency, and carbon conversion efficiency. Finally, the interchangeability for the syngas-natural blends is addressed.

2. Materials and methods

2.1. Feedstock

The experiments reported in this study used PKS and HVBC. Sieve analysis showed a particle size of PKS of 4.9 ± 2.3 mm (mean and standard deviation). The used HVBC was into the sieve fraction 4.7-9.5 mm. The moisture content of the air-dried PKS and HVBC amounted to 6.0 and 2.0 % wt, respectively.

2.2. Experimental setup

Figure 1 shows a side view of the TLUD gasifier, the gas sampling section, and the data acquisition system. The TLUD gasifier has an inner diameter of 152.4 mm, a height of 900 mm, and a 25 mm thick fiberglass thermal insulation layer (A detailed description of the TLUD setup used in this study can be found in a previous publication [1]). A blower supplies atmospheric air at the lower part of the

reactor. Before entering the reactor, the air passes through a manual control valve and a flow meter. The temperature data acquisition system includes six K-type thermocouples. The tip of each thermocouple reached the center of the bed.

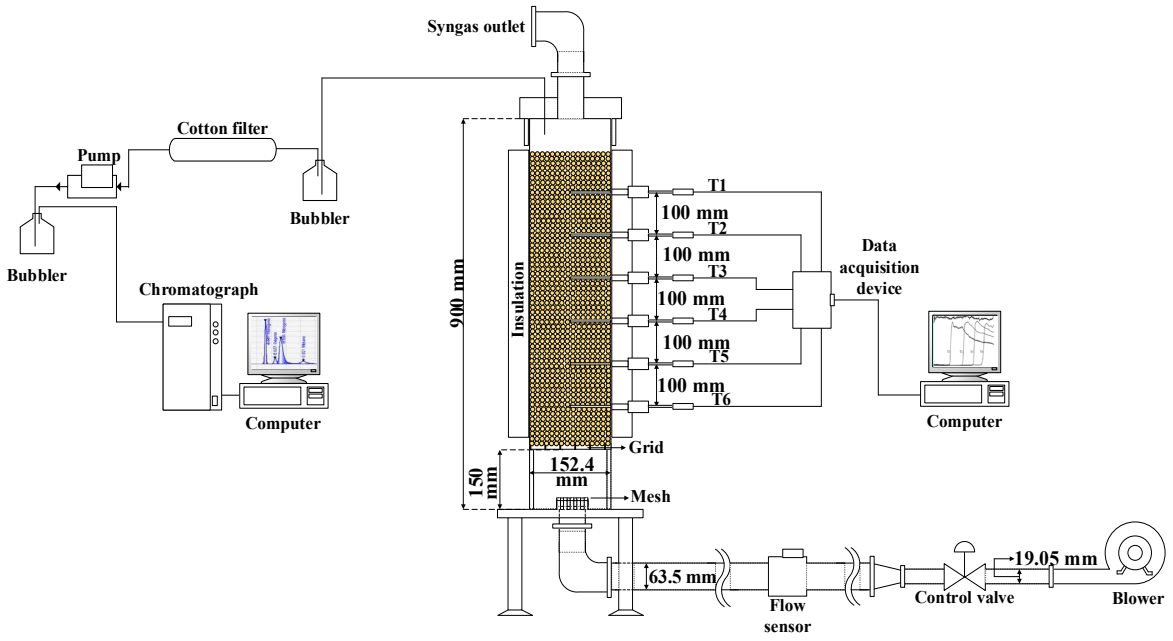

Figure 1. Schematic representation of the top-lit updraft (TLUD) fixed bed reactor setup.

2.3. Experimental conditions

The experimental variables were air superficial velocity (v_s), defined as the air volumetric flow divided by the cross-sectional area of the reactor, and coal volume percentage (VP_c). The measured temperature profiles and v_s enable the estimation of the ignition front propagation velocity (u_f). Equation 1 gives u_f as a function of the distance between consecutive thermocouples (Δx) and the time interval from the instance in which T_j reaches 500 °C until T_{j+1} reaches the same temperature ($t_{j+1} - t_j$). The equivalence ratio Φ, given by Equation 2, provides a first indication of the TLUD gasifier operation regime. Additionally, the measured syngas composition allows estimating energy content, cold gas efficiency (CGE), and carbon conversion efficiency (CCE). Table 1 shows the

operating conditions for the 3^2-factorial design of experiments. Analysis of the statistical significance of u_f can be found in the Supplementary Material.

$$u_f = \frac{\Delta x}{t_{j+1} - t_j} \quad \text{Eq. 1}$$

$$\Phi = \frac{AF}{AF_s} \quad \text{Eq. 2}$$

In Equation 2, AF and AF_s represent the actual and the stoichiometric air-fuel ratio, respectively. The calculation of AF requires the mass of converted fuel per unit time given by Equation 3, where A_T represents the cross-sectional area and ρ_b represents the bulk density of the bed. Note that AF_s depends on the elemental composition in Table 2 and the mass percentages of PKS and HVBC.

$$\dot{m}_f = u_f A_T \rho_b \quad \text{Eq. 3}$$

On the other hand, Equation 4 [44] gives the dry gas yield (Y) defined as the syngas production in Nm^3 per kg of solid fuel, where Q_a denotes the air volumetric flow, x_{Ash} is the ash content of feedstock in the proximate analysis, and y_{N_2} is the molar fraction of N_2 in the syngas. Mahapatro et al. [44] indicated that a high ash content of the feedstock impacts the dry gas yield estimation. Therefore, the high ash content of the coal used in our experiments requires estimating Y via Equation 4. Guangul et al. [45] and Gupta et al. [46] also used Equation 4 to estimate Y in the gasification of oil palm fronds and high-ash coal, respectively. Equations 5 and 6 allow calculating CGE and CCE, respectively. Note that LHV_g and LHV in Equation 5 are the lower heating value of the syngas and solid fuel in kJ Nm^{-3} and kJ kg^{-1}, respectively. In Equation 6, C is the mass percentage of atomic carbon in the feed, while y_{CO}, y_{CH_4}, and y_{CO_2} represent molar fractions in the syngas.

$$Y = \frac{0.79 Q_a}{\dot{m}_f \cdot (1 - x_{Ash}) \cdot y_{N_2}} \quad \text{Eq. 4}$$

$$CGE = Y \cdot \frac{\text{LHV}_\text{g}}{LHV} \cdot 100 \qquad \text{Eq. 5}$$

$$CCE = Y \cdot \frac{(y_{CO} + y_{CH_4} + y_{CO_2})}{C(22.4/12)} \cdot 100 \qquad \text{Eq. 6}$$

Equation 7 allows estimating the LHV_g [47] for syngas on a dry basis, where y_{CO}, y_{CH_4}, y_{H_2}, and y_{CO_2} represent molar fractions in syngas.

$$\text{LHV}_\text{g} = (30.0y_{CO} + 25.7y_{H_2} + 85.4y_{CH_4}) \times 0.0042 \text{ (MJ Nm}^{-3}\text{)} \qquad \text{Eq. 7}$$

Table 1. Experimental conditions for the 3^2-factorial design of experiments. Here, v_s represents air superficial velocity and VP_c coal volume percentage. Experiments named 1-1, 2-2, 3-3, and so on represent the initial experimental conditions and their replicate.

Experiment	v_s[a], m s^{-1}	VP_c, % v/v
1-1	0.096	15
2-2	0.082	30
3-3	0.069	15
4-4	0.082	0
5-5	0.096	0
6-6	0.096	30
7-7	0.069	30
8-8	0.069	0
9-9	0.082	15

[a]At normal conditions, 101.325 kPa and 15 °C

2.4. Gas Sampling

Syngas samples were collected every three minutes. First, the sample passed through a bubbling bottle, a cotton filter, and a vacuum pump. Next, the vacuum pump connected to a second bubbling bottle, in which the sample accumulated. Finally, from the second bubbling bottle, the sample entered the chromatographer through a sampling valve.

2.4.1. Gas Chromatography analysis

A micro-GC (Model 490, Agilent Technologies, Inc) was used to assess the syngas composition. The micro-GC has three channels, each one equipped with a thermal conductive detector (TCD). The first channel uses a CP-Molsieve 5A (10 m × 0.32 mm) column to quantify H_2, O_2, N_2, CH_4, and CO. The second channel includes a CP-PoraPLOT Q (10 m × 0.32 mm) column to quantify CO_2 and C_2H_6. Finally, the third channel uses a CP-Sil 5CB (8 m × 0.15 mm) column to quantify C_3H_8. Helium and Argon were the carrier gasses. Finally, well-defined mixtures (Linde S.A) were used for calibration. Triplicate runs with different concentrations provided the data to construct a quadratic calibration curve. Further details on the calibration mixtures and the Micro-GC setup can be found in the Supplementary Material.

2.5. Setup operation

The mass of PKS and HVBC for each blend was measured with a graduated cylinder. The particulate solids were blended for around two minutes before transferring them to the TLUD reactor. Thermocouples were introduced sequentially as the bed level rose to avoid the formation of empty pockets. After charging the reactor, v_s was increased gradually until reaching the prescribed value. Finally, the top layer of particulate solids was soaked in mineral diesel and ignited with a torch.

2.6. Gas interchangeability analysis

In this study, we estimate the interchangeability of the syngas via Delbourg's approach, which is used for the second family of gases (i.e., Natural Gas). Delbourg's approach assesses the possibility of replacing a combustible gas with another without changing the operating conditions in industrial or household burners. Moreover, Delbourg's method uses the Wobbe index and the combustion potential as parameters to evaluate the scope of the interchangeability. The Wobbe index (IW) indicates the gas energy content injected into a burner. Equation 7 gives IW, the ratio between the higher heating value of the gas and the square root of its relative density. Delbourg's approach defines a corrected

Wobbe index (IW_c), which corresponds to IW multiplied by the correction factors K_1 and K_2 in Equation 8 [48]. Factor K_1 is a function of the sum of the heating value of hydrocarbons having higher content than CH_4 [49]. Factor K_2 considers the Higher Heating Value of the syngas (HHV_g) and the CO, CO_2, and O_2 contents. Delbourg's approach also uses the combustion potential (C_{pot}) defined in Equation 9, which relates to the burning rate and combustion stability of the syngas produced. The ISO standard 13686:2013 contains several interchangeability methods, including Delbourg's approach [48].

$$IW = \frac{HHV_g}{\sqrt{d_r}} \quad \text{Eq. 7}$$

$$IW_c = K_1 K_2 IW \quad \text{Eq. 8}$$

$$C_{pot} = U\left(\frac{y_{H_2} + 0.7y_{CO} + 0.3y_{CH_4} + v\sum a y_{C_nH_m}}{\sqrt{dr}}\right) \quad \text{Eq. 9}$$

where d_r represents relative density, a is a correction coefficient for individual hydrocarbons, while U and v are correction factors considering the gas type [48]–[50]. Finally, $y_{C_nH_m}$ represents the molar fraction of hydrocarbons other than CH_4.

3. Results and discussion

3.1. Feedstock composition

The elemental compositions of PKS and HVBC differ notably on a dry-ash-free (daf) basis, as shown in Table 2. Compared with HVBC, PKS shows similar hydrogen (H) content, around 30% less carbon (C), and over twice as much oxygen (O). Nitrogen (N) and sulfur (S) together represent less than two percent of the daf mass of PKS and HVBC. Additionally, N content is higher in PKS, while S content is higher in HVBC. PKS contains less fixed carbon (FC) and over twice as much volatile matter (VM) as HVBC. A relatively high VM content indicates high reactivity in combustion applications, while FC correlates with the amount of char that remains after VM release. In addition, the ash content of

HVBC is notably higher. Finally, the HHV of PKS is lower than that of HVBC due to its higher O content.

Table 2 Elemental composition on a dry-ash-free basis (dafb), proximate analysis on a dry basis (db), and higher heating value (HHV) of the feedstock. VM represents volatile matter and FC fixed carbon.

Analysis/parameter	**Palm kernel shell, PKS** [51]	**High volatile bituminous coal, HVBC** [52]
C, % wt dafb	53.8	74.6
H, % wt dafb	6.13	6.07
N, % wt dafb	0.88	0.05
S, % wt dafb	0.11	1.91
O, % wt dafb	39.0	17.4
Molar H/C ratio	1.36	0.97
Molar O/C ratio	0.54	0.18
VM, % wt db	81.6	33.7
FC, % wt db	14.6	45.4
Ash, % wt db	3.78	20.9
HHV, kJ/kg db	21073[b]	25781[c]

[b]Gaur and Reed correlation [53], [c]Mason and Ghandi correlation [54].

3.2. Temperature profiles

Figure 2 shows the temperature profiles for each experiment and the corresponding air superficial velocity. Each temperature profile reflects a sudden and steep temperature increase caused by the downward-moving ignition front. Each temperature profile exhibits a peak and then decreases as the ignition front continues moving.

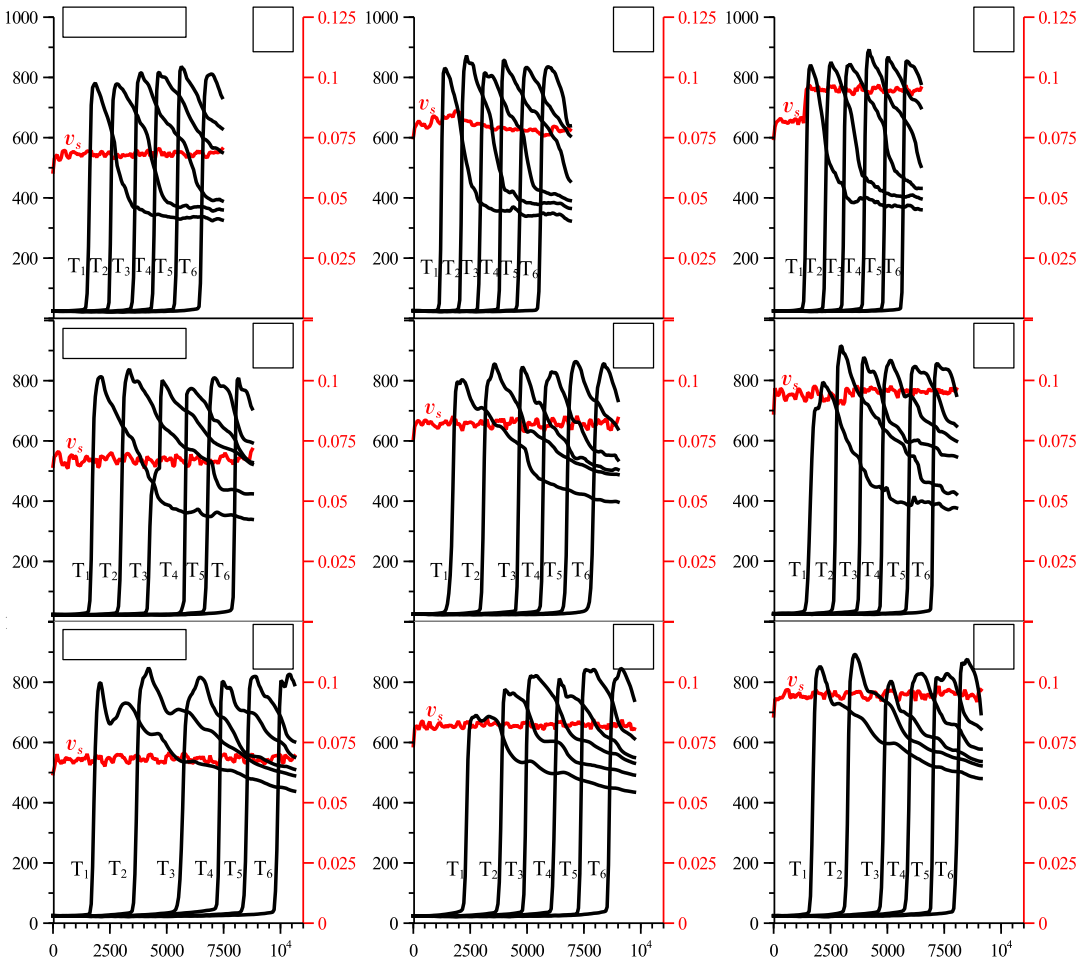

Figure 2. Temperature profiles for the top-lit updraft co-gasification of PKS and HVBC. Each column of figures corresponds to an air superficial velocity level: A, D, G 0.069 m s^{-1}, B, E, H 0.082 m $s^{-1,}$ and C, F, I 0.096 m s^{-1}. Each row of figures corresponds to the coal volume percentage indicated in A, D, and G.

Figure 2 shows that increasing v_s and decreasing VP_c lead to shorter batch times. The shorter reaction times for pure PKS are consistent with its relatively high VM content. The temperature profiles for the different experiments with pure PKS closely resemble each other, indicating a radially uniform consumption of PKS as the ignition front moves downward. The presence of HVBC delays the ignition front and causes significant variability in both temperature profiles and maximum

temperature. These results indicate that HVBC negatively affects the radial uniformity of the ignition front, which could be associated with differences between PKS and HVBC bulk densities that shift the positions of PKS and HVBC particles arbitrarily into the gasifier.

3.3. Ignition front propagation velocity

Figure 3 shows u_f and the maximum temperature T_m for each PKS-HVBC blend as a function of v_s. Each experimental run results in five u_f values, which were used together with the duplicate to calculate the average u_f value. T_m corresponds to the average of two values for each experimental condition. Pure PKS features significantly higher u_f values when compared with the PKS-HVBC blends. Increasing VP_c negatively affects u_f although the differences between 15% and 30% VP_c are less evident.

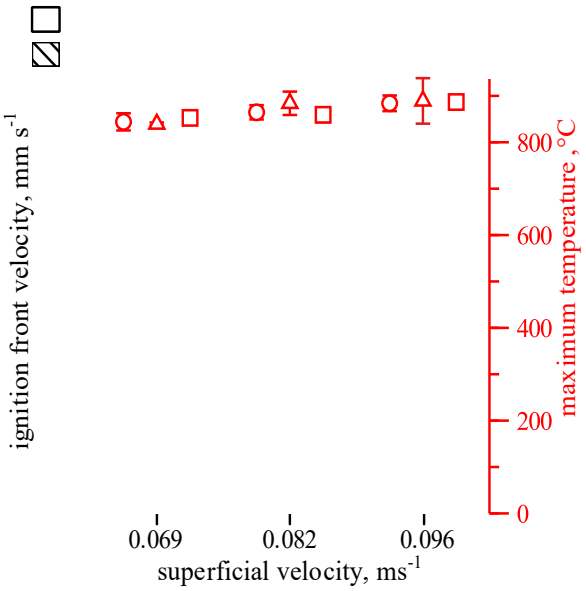

Figure 3. Ignition front propagation velocity (u_f) and maximum temperature (T_m) as a function of air superficial velocity (v_s) and coal volume percentage (VP_c). Columns and symbols, and their respective error bars, represent the mean and twice the standard deviation.

Results in Figure 3 are consistent with the lower bulk density and the higher reactivity of PKS. The lower variability in u_f for pure PKS provides further support to the ignition front's superior radial and axial uniformity compared with the blends. The differences in T_m between experiments was relatively low. Additionally, T_m increased slightly with v_s in all cases.

3.4. Equivalence ratio

Figure 4 shows the equivalence ratio (Φ) as a function of the v_s and VP_c. Results indicate that Φ remained in the range of 0.26 to 0.34 in all tests. A Φ value between 0.2 to 0.4 improves syngas production, while, Φ values higher than 0.4 could result in excessive CO_2, as pointed out in references [36][55].

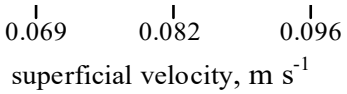

Figure 4. Equivalence ratio (Φ) as a function of the air superficial velocity (v_s) and coal volume percentage (VP_c). Columns and error bars correspond to the mean and twice the standard deviation.

Figure 4 shows a successive increase in Φ as v_s rises from 0.069 to 0.096 ms^{-1}, consistent with a higher amount of O_2 in the bed. The behavior of Φ relates to the u_f trends shown in Figure 3. Increasing u_f results in higher mass fuel consumption and lower values of the actual air-fuel ratio

(AF). On the other hand, the stoichiometric air-fuel ratio (AF_s) increases with VP_c because additional oxygen is required for complete combustion. As shown in Figure 4, Φ remained slightly constant at the low level of v_s, which indicates that the AF_s values for 0 %, 15 %, and 30 % vol of coal compensated the AF values. As v_s increased, Φ also increased and showed higher differences. This behavior could indicate that the differences between solid fuel bulk densities at higher v_s are more pronounced, which could shift the positions of PKS and HVBC particles in the gasifier, affecting the bed's void fraction. On the other hand, the high error bars (standard deviation) for 15 and 30 vol % of coal indicate a non-uniform ignition front, consistent with the difference in reactivity between HVBC and PKS.

3.5. Syngas composition

Figure 5 shows that increasing v_s caused only minor changes in the volume percentages of H_2, CO, CH_4, and CO_2. Aside from N_2, CO_2 had the highest share, followed by CO and H_2, while the CH_4 content was lower than 4.0 % vol. The composition of syngas is relatively uniform within the studied v_s and VP_c ranges. PKS can potentially act as a buffer again fluctuations in VP_c to maintain syngas quality. Only CO shows an average decrement of around 20% with increasing VP_c from 15 to 30. The scatter of the data does not allow to determine trends for the other syngas components, and this is not surprising given the relatively narrow v_s range. Likewise, the minor changes in the syngas compositions are also a consequence of the relatively close Φ values reached for the experimental conditions tested, which remained in the range of 0.26 to 0.34. James et al. [38] reported tar concentrations of about 2.76 g m^{-3} for rice husk and 11.8 g m^{-3} for wood chip gasification in a TLUD gasifier operating with air. In our study, we did not measure tar concentration in syngas. Tar concentration in syngas from biomass-coal mixtures in TLUD gasifiers, using air as a gasification agent, remains unexplored. Hence, further researches in our TLUD gasifier will include the tar measurement section, which could give insights into tar concentrations in syngas from biomass-coal mixtures.

The H_2/CO ratio indicates the syngas suitability for producing liquid fuel through, for example, the Fischer-Tropsch process [56]. Results obtained here show that the H_2/CO ratio remained in the range of 0.42-046, 0.49-0.51, and 0.57-0.59 for experiments with 0 %, 15 %, and 30 % vol HVBC, respectively. For chemical fuel derivation through the Fischer-Tropsch process, a stoichiometric H_2/CO ratio of 2 is required [56]. Using steam as the primary oxidizer increases the H_2 content in the syngas. Suitable H_2 contents in the syngas could also lead to applications in other industries as an alternative fuel reducing the greenhouse emissions from fossil fuels used in this industry. Note that these applications would be possible with an efficient H_2 storage process. The liquid Organic Hydrogen Carriers (LOHCs) method represents a promising route to hydrogen storage [57]. In our study, the syngas obtained can be used for direct heating in thermal applications without additional processing. As shown in Figure 5, the addition of coal results in higher H_2 and lower CO content, which agrees with results reported by Jeong et al. [23] in a fluidized bed reactor operating with air and at a bed temperature of 800°C. In their study [23], the H_2 content decreased by 47 % when the gasifier used pure biomass. The CO showed opposite results, increasing by 12 vol % at the same conditions. The above trends in H_2 and CO content resemble those obtained in this study.

On the other hand, Hernández et al. [27] indicate that the H_2/CO ratio increased as biomass in the blend raised from 0 to 100%. Furthermore, that study reports the co-gasification of dealcoholized grape marc and low-rank coal in an entrained flow gasifier with air. Moreover, the increase in the H_2/CO ratio was associated with biomass reactivity. In comparison, the H_2/CO ratios reached here are below those required in the Fischer-Tropsch process; nevertheless, future research in the co-gasification of PKS and HVBC in a TLUD gasifier should explore the addition of steam to increase the H_2/CO ratio.

Syngas compositions reported by Mallick et al. [24] show that the CO and CH_4 contents were higher for tests with pure biomass, which agrees with results obtained in our work for CO but contrasts with results for CH_4. Their study [24] used a circulating fluidized bed with air and bed temperatures in the

range of 700-900 °C. Likewise, Patel et al. [25] report an increase in the H_2 and CO_2 contents with an increase in the biomass share from 0 to 30% in a downdraft gasifier using air as the oxidizer. However, the CO and CH_4 contents remained constant. Again, these results were associated with high biomass reactivity, similar to that reported by Hernandez et al. [27]. High reactivity raises the temperature of the oxidation zone and promotes the Boudouard and steam reforming reactions. These CO_2 results agree with the results of our study, while the H_2 content presented an opposite trend.

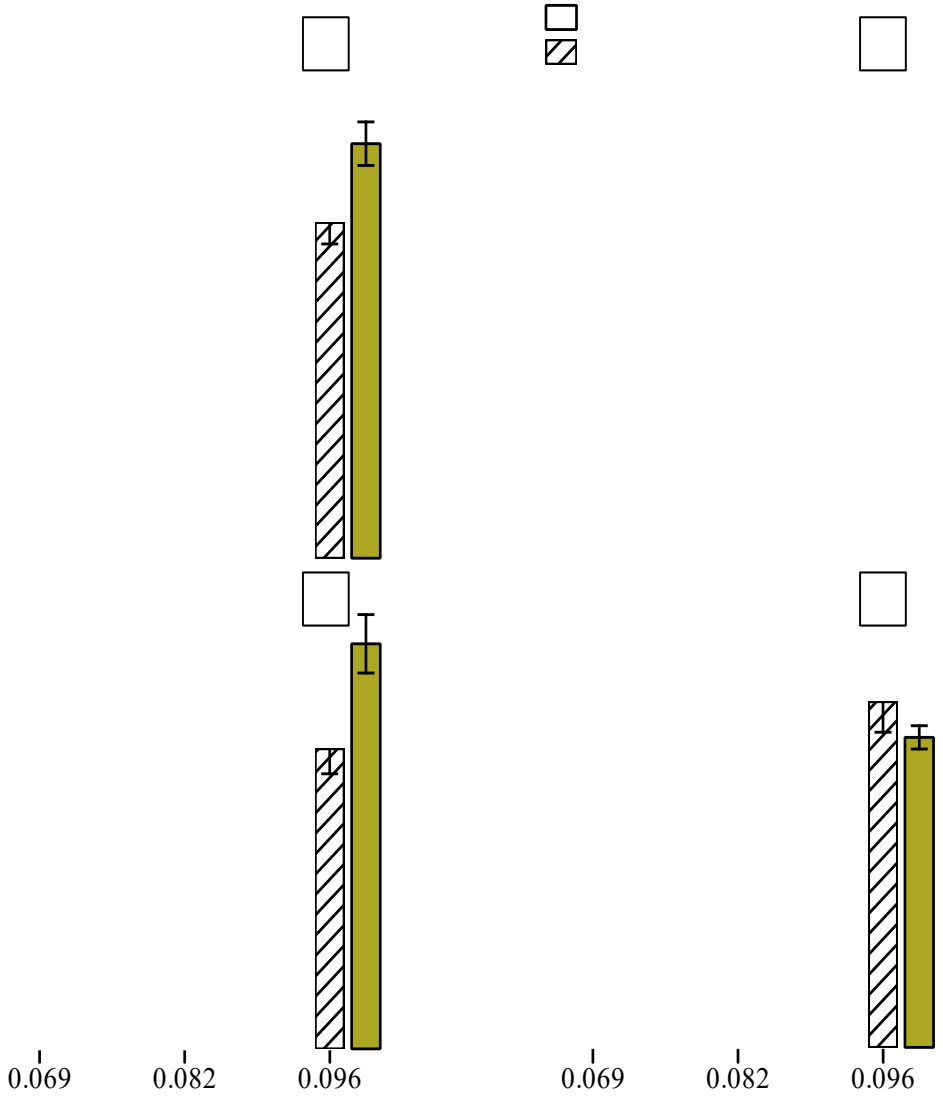

Figure 5. Syngas composition for the top-lit updraft co-gasification of PKS and HVBC. Volume percentage of the main syngas components: A) H_2, B) CO, C) CH_4, and D) CO_2 as a function of air superficial velocity (v_s) and coal volume percentage (VP_c). Columns and error bars correspond to the mean and twice the standard deviation, respectively.

3.6. Lower heating value (LHV_g) of the syngas.

In fixed bed reactors, typical LHV_g values lie in the range 4.0-5.6 MJ Nm^{-3} for downdraft and 3.7-5.1 MJ Nm^{-3} for (bottom lit) updraft operation [58][36]. Figure 6 shows only minor variations in LHV_g within the assessed v_s and VP_c ranges. Overall LHV_g is slightly higher for pure PKS, and the differences in LHV_g between the blends are indistinguishable because of the scatter of the data.

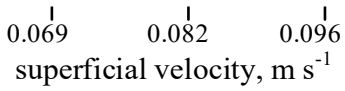

Figure 6. Lower heating value (LHV_g) as a function of air superficial velocity (v_s) and coal volume percentage (VP_c). Columns and error bars correspond to the mean and twice the standard deviation, respectively.

Tests with 100% PKS for v_s of 0.096 ms^{-1} produced the higher LHV_g with about 3.70 MJ Nm^{-3}. This value is similar to the LHV_g for 30 % vol HVBC and v_s at the higher level. Similarly, LHV_g for 15 %

vol HVBC did not show significant changes with the increase of v_s. Averaging, the LHV_g for pure PKS was 8% and 5% higher than 15 and 30 % vol HVBC. Similar results were observed in the downdraft gasifier operating with air by Sharma et al. [19] for 100% biomass. Likewise, Thengane et al. [59] reported that the LHV_g was higher (3.05 MJ m^{-3}) for tests with 75 % vol biomass and 25 % vol coal in a downdraft gasifier that used air. The above result was mainly associated with the higher volatiles and the catalytic effect of ash on biomass [59]. Opposite results were observed by Mahapatro et al. [44], who note that the LHV_g was higher for tests with 100% coal compared with sawdust and rice husk in a fluidized bed gasifier operating with air.

3.7. Cold gas and Carbon conversion efficiencies

Figure 7 illustrates how CGE and CCE vary with v_s and VP_c. The gas yield ranged from 1.98 to 3.26 m^3 kg^{-1}. CGE represents the ratio of the chemical energy of the syngas and the energy content of the solid fuel. In Figure 7, for 0% HVBC, CGE shows a linear increase from 34 to 46% with increasing v_s. For VP_c of 15%, CGE also increased from 35% to 45% as v_s was higher. For 30% of HVBC, the CGE remained almost constant (37%) for the low and intermediate levels of v_s, then increased (44%) for the high level of v_s. A plausible explanation for the almost constant behavior of CGE for v_s between 0.069 to 0.082m s^{-1} corresponds with a lower equivalence ratio reached for 30 % vol HVBC with the intermediate level of v_s. In addition, for 30% vol of coal, LHV of the PKS-HVBC blend is higher, which also causes a decrease in the CGE due to similar LHV_g values reached at this condition.

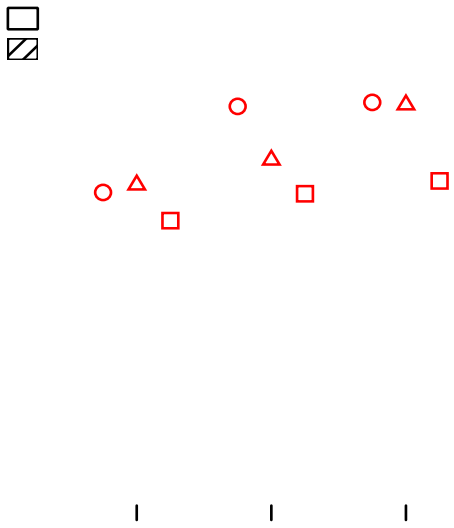

Figure 7. Cold gas efficiency (CGE) and Carbon conversion efficiency (CCE) as a function of the air superficial velocity (v_s) and coal volume percentage (VP_c).

Averaging, CGE for 0% and 15 % vol HVBC was 1.7% higher than that for 30 % vol HVBC. These results agree with those reported by Mallick et al. [24], who show a successive increase of CGE with Φ, and observe that CGE increased as the biomass share was higher in the co-gasification of coal and sawdust in a circulating fluidized bed.

With the increase of air superficial velocity, higher amounts of O_2 are available, thus enhancing CCE [24]. This result agrees with the trend observed in Figure 7, in which CCE increased with v_s. Tests with 0 % vol HVBC featured a higher carbon conversion efficiency. The above behavior is consistent with the observation of CO and CO_2 content shown in Figure 5, where pure PKS featured the higher concentration of these gases. For 15 % vol HVBC, CCE increased from 66 % to 83 % as v_s was higher, while 30 % vol HVBC produced the lowest CCE, reaching 59 % and 67 % for v_s between 0.069 and 0.096 mm s^{-1}, respectively. The results in Figure 7 highlight how the high reactivity of biomass enhances CCE. Moreover, blends with 15% of HVBC evidences how the high reactivity of the PKS improves the thermal conversion of the coal for the same experimental conditions, which

agrees with Thengane et al. [59]. Jeong et al. [23] also observe an increase in CCE with the rise of the biomass in the coal/biomass ratio for the co-gasification of coal and dried sewage sludge.

3.8. Gas interchangeability analysis

The corrected Wobbe Index and the combustion potential define the ordinate and the abscissa in the Delbourg diagram shown in Figure 8. Figure 8A shows six Natural gas-syngas blends. The syngas percentages lie in the range of 10-20 % vol. The reference natural gases used here, named NG_1 and NG_2, have a CH_4 content of 81.66 and 82.76 % vol, respectively. Those points within the boundary region defined by the dotted red line indicate a safe operation in natural gas burners working to atmospheric pressure. Figure 8A shows three blends inside the boundary region. Results suggest that a maximum of 15% and 10% vol of syngas blended with 85% vol NG_1 and 90% vol NG_2, respectively, could operate without problems in the atmospheric burner.

On the other hand, those points outside the boundary region are not interchangeable without modifications in the burner [50]. For example, if the blend points are to the left of the boundary region, the flame will quench, while if they locate to the right, the flame tends to decrease and then expire. Likewise, if the blend points are at the lower part of the boundary region, the blend combusts with excess air, reducing the burner's thermal power. In contrast, if the points are at the upper part of the boundary, the partial combustion of gas occurs [50].

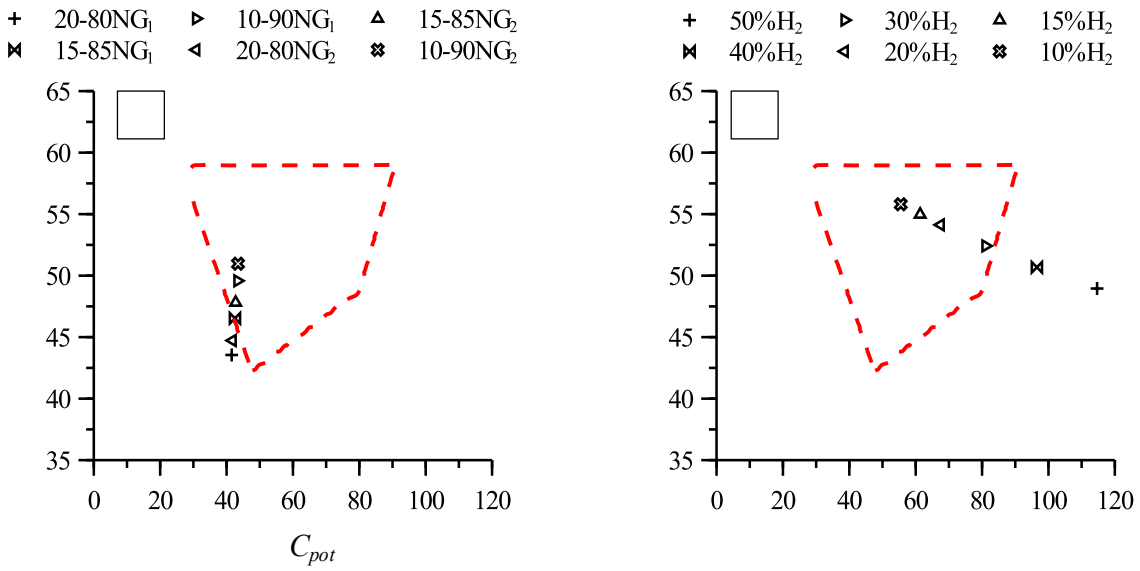

Figure 8. Delbourg diagram. A) Delbourg diagram for several blends of syngas and typical natural gases reported by Pulido et al. [60]. B) Delbourg diagram for H_2 and Natural gas (NG_2) blends. Each point indicates the operating region of the mixtures of syngas and natural gas for industrial or household burners. Diagrams were adapted from [50].

We carried out an additional interchangeability analysis by considering blends of Natural Gas and H_2 for the same natural gases tested above. The above scenario, associated with government policies for the energy transition towards an increase in the share of H_2 in the energy mix, in particular H_2 derived from the integration of renewable energies. Thus, the syngas could be targeted to maximize H_2 production, for example, via co-gasification using steam as the oxidizing agent. Figure 8B shows the results of this analysis. The aim was to determine the maximum H_2 percentage in the blends without causing operating problems in the burner. Increasing the use of the H_2 content in industrial applications decreases CO_2 emission. In addition, green hydrogen production increases the advantages of using H_2 as fuel in energetic systems. Likewise, the addition of H_2 derived from renewable energies into the Natural gas network could represent a viable means of storing excess wind and solar power [61]. However, further research is necessary to evaluate the performance of the combustion devices to avoid operating problems and remain secure.

Figure 8B shows that three blends formed by 20, 15, and 10 % vol of H_2 fall inside the operating region in the Delbourg diagram, indicating interchangeability without causing operational issues. The natural gas used in figure 8B is NG_2. The analysis for other natural gases by using identical H_2 percentages can be found in the Supplementary Material. The results indicate that 20% vol H_2 could operate in the natural gas burner successfully. Note that 30% H_2 locates close to the right boundary in Delbourg's diagram, which indicates that the combustion of the H_2-NG_2 blend could present inadequate functioning. Likewise, the supplementary material shows the same behavior for mixtures with other natural gases. For 20 % H_2 results agree with those reported by Vries et al. [61], who evaluate the interchangeability of the Natural gas and H_2 blends by considering the Wobbe index and the calculated flashback values for the formed mixtures. Their results indicate that 11.2 and 19.7% are H_2 contents that could operate without the risk of flashback. Further, the CH_4 content of the natural gases used by Vries et al. [61] ranged between 87 to 92.7 %.

4. Outlook

The abovementioned sections showed the operation of the TLUD gasifier for the co-gasification of coal and biomass. So far, this technology uses air as the principal oxidizer, with cookstoves in remote rural areas representing the main application. Further research in this technology could implement steam together with air as the oxidizers in the process. Furthermore, improving the syngas composition and continuous solids feeding could reveal additional advantages of this technology. In our previous study [1], the TLUD fixed-bed gasifier shows potential for a stable operation within a wide range of equivalence ratios with biomass-coal blends. In the gasification regimen, these results are confirmed, showing great potential to explore options that enhance the syngas quality. Likewise, different studies report the increase in syngas quality and the LHV via three main routes: air preheating, air and steam blends, and oxygen-enriched air as gasification agents. Air preheating combined with improved thermal insulation of the gasifier would enable the minimization of the equivalence ratio. For example, Guangul et al. [45] reported an increase in LHV from 4.7 to 5.3 MJ

Nm^{-3} when the air temperature changed from ambient conditions to 350 °C. Doherty et al. [62] and Wu et al. [63] also observed similar trends via gasification models. On the other hand, air-steam mixtures as gasification agents also improve syngas quality. Sharma et al. [64] reported an increase of H_2 and CO contents when steam was added into the reduction zone. Similar results were reported by Begum et al. [65] via simulation of the gasification process in Aspen Plus Software. On the contrary, Ngamchompoo et al. [66] indicated that the CO content decreased for steam-to-biomass ratios higher than 0.34. Using Oxygen-enriched air, Lenis et al. [67] reported an increase in u_f and the syngas LHV as the O_2 content was higher. These results were similar to those observed by Cao et al. [68] and Zhao et al. [69]. Coal-biomass blends affect the co-gasification process. However, due to the constant ash and char layer formed in this gasifier, further studies could explore the synergy effects of the ashes. For example, calcium and potassium contents present in biomass ash, together with the Iron, Nickel, and Zinc contents of coal ash, could act as catalysts in the co-gasification process [27], enhancing, among other variables, the syngas quality.

Syngas originating from the co-gasification of coal and biomass can potentially form mixtures with natural gas for co-processing in combustion processes. Gas interchangeability represents a suitable route to tackle the variations in the chemical composition of natural gases. In addition, this method serves as a bridge to explore gas mixtures from other sources such as plastic gasification or pyrolysis, manufactured gases, biogas, among others. Burner manufacturers will need to design these devices to tolerate a broad range of operating conditions, thus covering gases with variable chemical compositions.

Increasing syngas production via the co-gasification process could alleviate natural gas depletion. However, to reach a suitable gas production, it is urgent to increase the syngas energy content. Further, such an improvement would allow rising the syngas percentage in blends with natural gas for combustion applications. Therefore, syngas- and H_2 enriched-natural gas could be the drivers to reach a reliable and affordable energy supply.

5. Conclusions

Biomass and coal co-gasification produce syngas with energetic properties suitable for co-firing with natural gas in diverse applications. The co-gasification process takes advantage of the renewable nature and high reactivity of biomass, and the availability of coal, together with its high energy content. This study presents an experimental study of this process in a TLUD fixed bed gasifier, a reactor where the ignition front begins on the top and then shift to the bottom while the gas product flows upwards. We developed A 3^2 factorial design to evaluate the effect of the air superficial velocity and the PKS-HVBC blends on the u_f and syngas quality in the biomass and coal co-gasification. The u_f and syngas quality allowed characterizing the behavior of parameters such as LHV_g, CGE, and CCE in the co-gasification process. The experimental tests were restricted to the gasification regimen in the TLUD gasifier, evidencing the great potential of this reactor for the co-gasification of PKS and HVBC. The study finalizes exploring an interchangeability analysis between syngas, H_2, and several natural gases. Results derived from the above analysis showed that the syngas could combust in atmospheric natural gas burners without modifications.

The results indicate slight differences in the syngas compositions with PKS-HVBC blends and the successive increase of v_s. This behavior agrees with the relatively short range of variation in the equivalence ratio (0.26 to 0.34) for the gasification regimen of the TLUD gasifier. H_2 and CH_4 increased as the coal percentage was higher, while CO and CO_2 raised with the increase of the PKS. VP_c of 0% produced the higher LHV_g, this trend is associated with the high CO content obtained for 100% PKS, which presented a 20 % higher CO than tests with 15 and 30% of VP_c. CGE and CCE followed the same trend, i.e., they are higher for VP_c of 0%, which agrees with the high LHV_g, and CO and CO_2 values obtained in this study. The higher LHV_g of the syngas was used in the gas interchangeability analysis. The results indicate that 10 and 15% vol of the syngas obtained by co-gasification of PKS and HVBC could use with some reference natural gasses in industrial or household burner applications based on Delbourg's approach. Moreover, the trend indicates that if

the syngas energy content was higher, more syngas could be blended with natural gas. This analysis shows the feasibility of syngas integration obtained by co-gasification of PKS and HVBC in industrial applications.

Acknowledgments

MINCIENCIAS supported this work through the Ph.D. National Scholarship Becas Bicentenario 2019 Contract UN-OJ-2020-47414. This work was also supported by "Convocatoria 753 para la formación de capital humano de alto nivel para el Departamento Norte de Santander".

References

[1] D. A. Quintero-Coronel, Y. A. Lenis-Rodas, L. A. Corredor, P. Perreault, and A. Gonzalez-Quiroga, “Thermochemical conversion of coal and biomass blends in a top-lit updraft fixed bed reactor: Experimental assessment of the ignition front propagation velocity,” *Energy*, vol. 220, p. 119702, 2021, doi: 10.1016/j.energy.2020.119702.

[2] M. Markovic, E. A. Bramer, and G. Brem, “Experimental investigation of wood combustion in a fixed bed with hot air,” *Waste Manag.*, vol. 34, no. 1, pp. 49–62, 2014, doi: 10.1016/j.wasman.2013.09.021.

[3] C. Yin, L. A. Rosendahl, and S. K. Kær, “Grate-firing of biomass for heat and power production,” *Prog. Energy Combust. Sci.*, vol. 34, no. 6, pp. 725–754, 2008, doi: https://doi.org/10.1016/j.pecs.2008.05.002.

[4] C. Ryu, A. N. Phan, Y. bin Yang, V. N. Sharifi, and J. Swithenbank, “Ignition and burning rates of segregated waste combustion in packed beds,” *Waste Manag.*, vol. 27, no. 6, pp. 802–810, 2007, doi: 10.1016/j.wasman.2006.04.013.

[5] C. S. Pereira and B. A. Patel, “The role of process intensification in addressing the dual energy challenge,” *Chem. Eng. Process. - Process Intensif.*, vol. 142, no. May, p. 107545, 2019, doi:

10.1016/j.cep.2019.107545.

[6] Z. Ong *et al.*, "Co-gasification of woody biomass and sewage sludge in a fixed-bed downdraft gasifier," *AIChE J.*, vol. 61, no. 8, pp. 2508–2521, Aug. 2015, doi: 10.1002/aic.14836.

[7] P. Kuo and W. Wu, "Design of co-gasification from coal and biomass combined heat and power generation system," *Energy Procedia*, vol. 75, pp. 1120–1125, 2015, doi: 10.1016/j.egypro.2015.07.523.

[8] B. P. S. Review and W. E. June, "BP Statistical Review of World Energy," 2019.

[9] UPME and MINMINAS, "Integración de las Energías Renovables No Convencionales en Colombia," 2015.

[10] UPME, *Atlas del Potencial Energético de la Biomasa Residual en Colombia*, vol. 95, no. 1155. UPME, 2009.

[11] R. Razuan, Q. Chen, X. Zhang, V. Sharifi, and J. Swithenbank, "Pyrolysis and combustion of oil palm stone and palm kernel cake in fixed-bed reactors," *Bioresour. Technol.*, vol. 101, no. 12, pp. 4622–4629, 2010, doi: 10.1016/j.biortech.2010.01.079.

[12] F. P. Arrieta, E. S. Lora, E. Yáñez, and E. Castillo, "Potencial de cogeneración de energía eléctrica en la agroindustria colombiana de aceite de palma: tres estudios de casos," *PALMAS*, vol. 29, no. 4, pp. 59–73, 2008.

[13] P. M. Briceño Álvarez Ivonne Cristina, Valencia Concha Jaime Fernando, "Potencial de generación de energía de la agroindustria de la palma de aceite en Colombia," *Rev. Palmas*, vol. 36, no. 3, pp. 43–53, 2015.

[14] D. A. Ali, M. A. Gadalla, O. Y. Abdelaziz, C. P. Hulteberg, and F. H. Ashour, "Co-gasification of coal and biomass wastes in an entrained flow gasifier: Modelling, simulation and integration opportunities," *J. Nat. Gas Sci. Eng.*, vol. 37, pp. 126–137, 2017, doi:

10.1016/j.jngse.2016.11.044.

[15] C. Van Huynh and S. C. Kong, “Combustion and NOx emissions of biomass-derived syngas under various gasification conditions utilizing oxygen-enriched-air and steam,” *Fuel*, vol. 107, no. x, pp. 455–464, 2013, doi: 10.1016/j.fuel.2012.12.016.

[16] C. F. Valdés *et al.*, “Co-gasification of sub-bituminous coal with palm kernel shell in fluidized bed coupled to a ceramic industry process,” *Appl. Therm. Eng.*, vol. 107, pp. 1201–1209, 2016, doi: 10.1016/j.applthermaleng.2016.07.086.

[17] A. D. Kamble, V. K. Saxena, P. D. Chavan, and V. A. Mendhe, “Co-gasification of coal and biomass an emerging clean energy technology: Status and prospects of development in Indian context,” *Int. J. Min. Sci. Technol.*, vol. 29, no. 2, pp. 171–186, 2019, doi: 10.1016/j.ijmst.2018.03.011.

[18] I. Aigner, C. Pfeifer, and H. Hofbauer, “Co-gasification of coal and wood in a dual fluidized bed gasifier,” *Fuel*, vol. 90, no. 7, pp. 2404–2412, 2011, doi: 10.1016/j.fuel.2011.03.024.

[19] M. Sharma, S. Attanoor, and S. Dasappa, “Investigation into co-gasifying Indian coal and biomass in a down draft gasifier - Experiments and analysis,” *Fuel Process. Technol.*, vol. 138, pp. 435–444, 2015, doi: 10.1016/j.fuproc.2015.06.015.

[20] J. S. Brar, K. Singh, J. Wang, and S. Kumar, “Cogasification of Coal and Biomass: A Review,” *Int. J. For. Res.*, vol. 2012, pp. 1–10, 2012, doi: 10.1155/2012/363058.

[21] M. Horttanainen, J. Saastamoinen, and P. Sarkomaa, “Operational limits of ignition front propagation against airflow in packed beds of different wood fuels,” *Energy and Fuels*, vol. 16, no. 3, pp. 676–686, 2002, doi: 10.1021/ef010209d.

[22] H. M. Yoo, J. S. Lee, W. S. Yang, H. S. Choi, H. N. Jang, and Y. C. Seo, “Co-gasification characteristics of palm oil by-products and coals for syngas production,” *Korean J. Chem.*

Eng., vol. 35, no. 3, pp. 654–661, 2018, doi: 10.1007/s11814-017-0312-x.

[23] Y. S. Jeong, Y. K. Choi, K. B. Park, and J. S. Kim, "Air co-gasification of coal and dried sewage sludge in a two-stage gasifier: Effect of blending ratio on the producer gas composition and tar removal," *Energy*, vol. 185, pp. 708–716, 2019, doi: 10.1016/j.energy.2019.07.093.

[24] D. Mallick, P. Mahanta, and V. S. Moholkar, "Co–gasification of coal/biomass blends in 50 kWe circulating fluidized bed gasifier," *J. Energy Inst.*, vol. 93, no. 1, pp. 99–111, 2020, doi: 10.1016/j.joei.2019.04.005.

[25] V. R. Patel, D. Patel, N. S. Varia, and R. N. Patel, "Co-gasification of lignite and waste wood in a pilot-scale (10kWe) downdraft gasifier," *Energy*, vol. 119, pp. 834–844, 2017, doi: 10.1016/j.energy.2016.11.057.

[26] K. Kumabe, T. Hanaoka, S. Fujimoto, T. Minowa, and K. Sakanishi, "Co-gasification of woody biomass and coal with air and steam," vol. 86, pp. 684–689, 2007, doi: 10.1016/j.fuel.2006.08.026.

[27] J. J. Hernández, G. Aranda-Almansa, and C. Serrano, "Co-gasification of biomass wastes and coal-coke blends in an entrained flow gasifier: An experimental study," *Energy and Fuels*, vol. 24, no. 4, pp. 2479–2488, 2010, doi: 10.1021/ef901585f.

[28] H. E. Díez and J. F. Pérez, "Effects of wood biomass type and airflow rate on fuel and soil amendment properties of biochar produced in a top-lit updraft gasifier," *Environ. Prog. Sustain. Energy*, vol. 38, no. 4, pp. 1–14, 2019, doi: 10.1002/ep.13105.

[29] F. V. Tinaut, A. Melgar, J. F. Pérez, and A. Horrillo, "Effect of biomass particle size and air superficial velocity on the gasification process in a downdraft fixed bed gasifier. An experimental and modelling study," *Fuel Process. Technol.*, vol. 89, no. 11, pp. 1076–1089, 2008, doi: 10.1016/j.fuproc.2008.04.010.

[30] T. Kirch, P. R. Medwell, C. H. Birzer, and P. J. van Eyk, “Small-scale autothermal thermochemical conversion of multiple solid biomass feedstock,” *Renew. Energy*, vol. 149, pp. 1261–1270, 2020, doi: 10.1016/j.renene.2019.10.120.

[31] T. Kirch, P. R. Medwell, C. H. Birzer, and P. J. van Eyk, “Influences of Fuel Bed Depth and Air Supply on Small-Scale Batch-Fed Reverse Downdraft Biomass Conversion,” *Energy & Fuels*, vol. 32, no. 8, pp. 8507–8518, Aug. 2018, doi: 10.1021/acs.energyfuels.8b01699.

[32] S. Varunkumar, N. K. S. Rajan, and H. S. Mukunda, “Universal flame propagation behavior in packed bed of biomass,” *Combust. Sci. Technol.*, vol. 185, no. 8, pp. 1241–1260, 2013, doi: 10.1080/00102202.2013.782297.

[33] M. Fatehi and M. Kaviany, “Adiabatic reverse combustion in a packed bed,” *Combust. Flame*, vol. 99, no. 1, pp. 1–17, 1994, doi: 10.1016/0010-2180(94)90078-7.

[34] C. Steiner *et al.*, “Participatory trials of on-farm biochar production and use in Tamale, Ghana,” *Agron. Sustain. Dev.*, vol. 38, no. 1, 2018, doi: 10.1007/s13593-017-0486-y.

[35] Y. A. Lenis, A. F. Agudelo, and J. F. Pérez, “Analysis of statistical repeatability of a fixed bed downdraft biomass gasification facility,” *Appl. Therm. Eng.*, vol. 51, no. 1–2, pp. 1006–1016, 2013, doi: 10.1016/j.applthermaleng.2012.09.046.

[36] A. Saravanakumar, T. M. Haridasan, T. B. Reed, and R. K. Bai, “Experimental investigation and modelling study of long stick wood gasification in a top lit updraft fixed bed gasifier,” *Fuel*, vol. 86, no. 17–18, pp. 2846–2856, 2007, doi: 10.1016/j.fuel.2007.03.028.

[37] R. A. M. James, W. Yuan, and M. D. Boyette, “The effect of biomass physical properties on top-lit updraft gasification of woodchips,” *Energies*, vol. 9, no. 4, 2016, doi: 10.3390/en9040283.

[38] A. M. James R, W. Yuan, M. D. Boyette, and D. Wang, “Airflow and insulation effects on

simultaneous syngas and biochar production in a top-lit updraft biomass gasifier," *Renew. Energy*, vol. 117, pp. 116–124, 2018, doi: 10.1016/j.renene.2017.10.034.

[39] D. Shin and S. Choi, "The combustion of simulated waste particles in a fixed bed," *Combust. Flame*, vol. 121, no. 1, pp. 167–180, 2000, doi: https://doi.org/10.1016/S0010-2180(99)00124-8.

[40] Y. B. Yang, V. N. Sharifi, and J. Swithenbank, "Effect of air flow rate and fuel moisture on the burning behaviours of biomass and simulated municipal solid wastes in packed beds," *Fuel*, vol. 83, no. 11–12, pp. 1553–1562, 2004, doi: 10.1016/j.fuel.2004.01.016.

[41] M. R. Karim and J. Naser, "Numerical study of the ignition front propagation of different pelletised biomass in a packed bed furnace," *Appl. Therm. Eng.*, vol. 128, pp. 772–784, 2018, doi: 10.1016/j.applthermaleng.2017.09.061.

[42] Y. Mehta and C. Richards, "Gasification performance of a top-lit updraft cook stove," *Energies*, vol. 10, no. 10, 2017, doi: 10.3390/en10101529.

[43] J. F. Pérez, A. Melgar, and P. N. Benjumea, "Effect of operating and design parameters on the gasification/combustion process of waste biomass in fixed bed downdraft reactors: An experimental study," *Fuel*, vol. 96, pp. 487–496, 2012, doi: 10.1016/j.fuel.2012.01.064.

[44] A. Mahapatro and P. Mahanta, "Gasification studies of low-grade Indian coal and biomass in a lab-scale pressurized circulating fluidized bed," *Renew. Energy*, vol. 150, pp. 1151–1159, 2019, doi: 10.1016/j.renene.2019.10.038.

[45] F. M. Guangul, S. A. Sulaiman, and A. Ramli, "Gasifier selection, design and gasification of oil palm fronds with preheated and unheated gasifying air," *Bioresour. Technol.*, vol. 126, pp. 224–232, 2012, doi: 10.1016/j.biortech.2012.09.018.

[46] S. Gupta and S. De, "An experimental investigation of high-ash coal gasification in a pilot-

scale bubbling fluidized bed reactor," *Energy*, p. 122868, 2021, doi: https://doi.org/10.1016/j.energy.2021.122868.

[47] P. M. Lv, Z. H. Xiong, J. Chang, C. Z. Wu, Y. Chen, and J. X. Zhu, "An experimental study on biomass air-steam gasification in a fluidized bed," *Bioresour. Technol.*, vol. 95, no. 1, pp. 95–101, 2004, doi: 10.1016/j.biortech.2004.02.003.

[48] ISO, *ISO 13686:2013 Natural gas — Quality designation*, vol. 2013. 2013, p. 48.

[49] S. Honus, S. Kumagai, O. Němček, and T. Yoshioka, "Replacing conventional fuels in USA, Europe, and UK with plastic pyrolysis gases – Part I: Experiments and graphical interchangeability methods," *Energy Convers. Manag.*, vol. 126, pp. 1118–1127, 2016, doi: 10.1016/j.enconman.2016.08.055.

[50] S. Honus, D. Juchelkova, A. Campen, and T. Wiltowski, "Gaseous components from pyrolysis - Characteristics, production and potential for energy utilization," *J. Anal. Appl. Pyrolysis*, vol. 106, pp. 1–8, 2014, doi: 10.1016/j.jaap.2013.11.023.

[51] A. Verdeza-Villalobos, Y. A. Lenis-Rodas, A. J. Bula-Silvera, J. M. Mendoza-Fandiño, and R. D. Gómez-Vásquez, "Performance analysis of a commercial fixed bed downdraft gasifier using palm kernel shells," *CTyF - Ciencia, Tecnol. y Futur.*, vol. 9, no. 2, pp. 79–88, 2019, doi: 10.29047/01225383.181.

[52] R. B. Zapata, J. F. P. Bayer, and C. S. Jiménez, "Carbones colombianos: clasificación y caracterización termoquímica para aplicaciones energéticas," *Rev. ION*, vol. 27, no. 2, pp. 43–54, 2014.

[53] S. Gaur and T. B. T. B. Reed, "An atlas of thermal data for biomass and other fuels," *Nrel*. National Renewable Energy Lab., Golden, CO (United States), pp. 1–189, 1995.

[54] D. M. Mason and K. N. Gandhi, "Formulas for calculating the calorific value of coal and coal

chars: Development, tests, and uses," *Fuel Process. Technol.*, vol. 7, no. 1, pp. 11–22, 1983, doi: https://doi.org/10.1016/0378-3820(83)90022-X.

[55] A. A. P. Susastriawan, H. Saptoadi, and Purnomo, "Design and experimental study of pilot scale throat-less downdraft gasifier fed by rice husk and wood sawdust," *Int. J. Sustain. Energy*, vol. 37, no. 9, pp. 873–885, 2018, doi: 10.1080/14786451.2017.1383992.

[56] Y. Cao *et al.*, "Synthesis gas production with an adjustable H2/CO ratio through the coal gasification process: Effects of coal ranks and methane addition," *Energy and Fuels*, vol. 22, no. 3, pp. 1720–1730, 2008, doi: 10.1021/ef7005707.

[57] L. Van Hoecke, L. Laffineur, R. Campe, P. Perreault, S. W. Verbruggen, and S. Lenaerts, "Challenges in the use of hydrogen for maritime applications," *Energy Environ. Sci.*, vol. 14, no. 2, pp. 815–843, 2021, doi: 10.1039/d0ee01545h.

[58] N. Couto, A. Rouboa, V. Silva, E. Monteiro, and K. Bouziane, "Influence of the biomass gasification processes on the final composition of syngas," in *Energy Procedia*, 2013, vol. 36, pp. 596–606, doi: 10.1016/j.egypro.2013.07.068.

[59] S. K. Thengane, A. Gupta, and S. M. Mahajani, "Co-gasification of high ash biomass and high ash coal in downdraft gasifier," *Bioresour. Technol.*, vol. 273, no. November, pp. 159–168, 2019, doi: 10.1016/j.biortech.2018.11.007.

[60] O. Barreto, "Comparación del desempeño de varias calidades de gas natural y evaluación de viabilidad para el uso de biogás como combustible para vehículos que operan con GNCV," *Univ. Nac. Colomb.*, pp. 1–112, 2017, [Online]. Available: https://repositorio.unal.edu.co/handle/unal/59902.

[61] H. de Vries, A. V. Mokhov, and H. B. Levinsky, "The impact of natural gas/hydrogen mixtures on the performance of end-use equipment: Interchangeability analysis for domestic

appliances," *Appl. Energy*, vol. 208, no. September, pp. 1007–1019, 2017, doi: 10.1016/j.apenergy.2017.09.049.

[62] W. Doherty, A. Reynolds, and D. Kennedy, "The effect of air preheating in a biomass CFB gasifier using ASPEN Plus simulation," *Biomass and Bioenergy*, vol. 33, no. 9, pp. 1158–1167, 2009, doi: 10.1016/j.biombioe.2009.05.004.

[63] K. T. Wu and R. Y. Chein, "Modeling of Biomass Gasification with Preheated Air at High Temperatures," *Energy Procedia*, vol. 75, pp. 214–219, 2015, doi: 10.1016/j.egypro.2015.07.307.

[64] S. Sharma and P. N. Sheth, "Air-steam biomass gasification: Experiments, modeling and simulation," *Energy Convers. Manag.*, vol. 110, pp. 307–318, 2016, doi: 10.1016/j.enconman.2015.12.030.

[65] S. Begum, M. G. Rasul, D. Akbar, and D. Cork, "An experimental and numerical investigation of fluidized bed gasification of solid waste," *Energies*, vol. 7, no. 1, pp. 43–61, 2014, doi: 10.3390/en7010043.

[66] W. Ngamchompoo and K. Triratanasirichai, "Experimental investigation of high temperature air and steam biomass gasification in a fixed-bed downdraft gasifier," *Energy Sources, Part A Recover. Util. Environ. Eff.*, vol. 39, no. 8, pp. 733–740, 2017, doi: 10.1080/15567036.2013.783657.

[67] Y. A. Lenis, J. F. Pérez, and A. Melgar, "Fixed bed gasification of Jacaranda Copaia wood : Effect of packing factor and oxygen enriched air," *Ind. Crop. Prod.*, vol. 84, pp. 166–175, 2016, doi: 10.1016/j.indcrop.2016.01.053.

[68] Y. Cao, Q. Wang, J. Du, and J. Chen, "Oxygen-enriched air gasification of biomass materials for high-quality syngas production," *Energy Convers. Manag.*, vol. 199, no. September, 2019,

doi: 10.1016/j.enconman.2019.05.054.

[69] J. Zhao *et al.*, “Hydrogen-rich syngas produced from co-gasification of municipal solid waste and wheat straw in an oxygen-enriched air fluidized bed,” *Int. J. Hydrogen Energy*, vol. 46, no. 34, pp. 18051–18063, 2021, doi: 10.1016/j.ijhydene.2021.02.137.